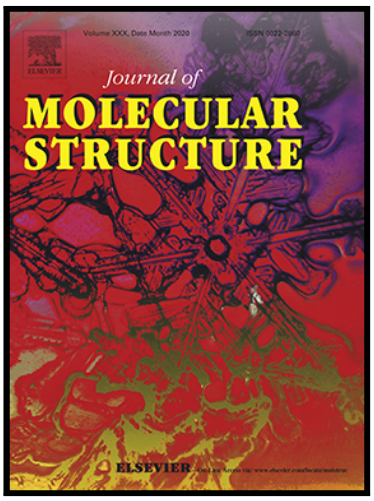

Synthesis, structural characterization, Hirshfeld surface analysis and in vitro-antimicrobial activities of triphenyltin (IV) compounds of azo-carboxylates derived from 2- or 4-amino benzoic acids and naphthalen-1 or 2-ol

Paresh Debnath , Keisham Surjit Singh , Swatika Sharma , Pratima Debnath , S.Sureshkumar Singh , Les law Sieroń , Waldemar Maniukiewicz

PII: S0022-2860(20)31295-3
DOI: https://doi.org/10.1016/j.molstruc.2020.128971
Reference: MOLSTR 128971

To appear in: *Journal of Molecular Structure*

Received date: 16 May 2020
Revised date: 23 July 2020
Accepted date: 24 July 2020

Please cite this article as: Paresh Debnath , Keisham Surjit Singh , Swatika Sharma , Pratima Debnath , S.Sureshkumar Singh , Les law Sieroń , Waldemar Maniukiewicz , Synthesis, structural characterization, Hirshfeld surface analysis and in vitro-antimicrobial activities of triphenyltin (IV) compounds of azo-carboxylates derived from 2- or 4-amino benzoic acids and naphthalen-1 or 2-ol, *Journal of Molecular Structure* (2020), doi: https://doi.org/10.1016/j.molstruc.2020.128971

Highlights

- Three triphenyltin(IV) compounds **1-3** were synthesized and characterized.
- **1** showed intermediate between distorted TBP and square-pyramidal geometry.
- **3** exhibited distorted tetrahedral geometry with monomeric structure.
- Hirshfield surfaces analysis of **1** and **3** observed different stacking interactions.
- Compounds were isostructural and adopted four coordinated structure in solution.
- Compounds showed significant antimicrobial activity.

Synthesis, structural characterization, Hirshfeld surface analysis and *in vitro*-antimicrobial activities of triphenyltin (IV) compounds of azo-carboxylates derived from 2- or 4-amino benzoic acids and naphthalen-1 or 2-ol

Paresh Debnath[a], Keisham Surjit Singh[a,d*], Swatika Sharma[b], Pratima Debnath[a], S.Sureshkumar Singh[b], Lesław Sieroń[c], Waldemar Maniukiewicz[c*]

[a]*Department of Chemistry, National Institute of Technology Agartala, Jirania, Tripura (west)-799046, India*

[b]*Department of Forestry, North Eastern Regional Institute of Science And Technology, Nirjuli, Arunachal Pradesh -791109, India*

[c] *Institute of General and Ecological Chemistry, Lodz University of Technology, 90-924 Lodz, Zeromskiego 116, Poland*

[d]*Department of Chemistry, Manipur University, Canchipur -795003, Imphal, Manipur, India*

Abstract

Synthesis of three new triphenyltin (IV) compounds **1**-**3** were reported by the reaction of azo-carboxylic acid ligands *viz.*2/4-(2-hydroxynaphthylazo)-benzoic acids [compounds **1** and **2**] or 2-(4-hydroxynaphthylazo)-benzoic acid [compound **3]** with triphenyltin(IV) hydroxide. The compounds were completely characterized with the help of elemental analysis, IR and multinuclear [^{1}H, ^{13}C and ^{119}Sn]-NMR spectroscopy. The mode of coordination and geometry around tin atoms in compounds **1** and **3** were determined by X-ray crystallography. Compounds **1** and **3** exhibited monomeric structure with intermediate deformation between the trigonal bipyramidal and square-pyramidal geometry or distorted tetrahedral geometry around tin atom respectively. Hirshfeld surface analysis for both structures was also performed. The main difference between **1** and **3** is observed for stacking interactions. ^{119}Sn NMR spectral study of all the compounds suggested that the compounds adopted 4-coordinated tetrahedral structures in solution. The antimicrobial activities of the compounds showed effective antibacterial activity against *S. aureus* and antifungal activity against *F. oxysporum*. The antimicrobial activity of these compounds was found to be higher than the tested standard compounds against some selected microbes.

Key Words Triphenyltin(IV) complexes; crystal structures; Hirshfeld surfaces; NMR spectroscopy; antimicrobial activities.

Corresponding authors:**E-mail address*: surjitkeisham@yahoo.co.in, keishamchem@gmail.com (KSS), waldemar.maniukiewicz@p.lodz.pl (WM)

1. Introduction

Chemistry of organotin (IV) carboxylates have been studied considerably for the last few decades in organotin chemistry because of their interesting versatile molecular structures exhibited as monomeric, dimeric, tetrameric, polymeric, hexagonal drum, ladder, macro-cyclic and macro-cyclic porous structures [1-7]. Moreover, organotin (IV) carboxylates were also investigated for the search of their possible biological applications. For instance they were found to exhibit important biological properties such as anti-proliferation, antibacterial, cytotoxicity, anti-tuberculosis and anticancer agents etc. [8-12] Similarly, attention have also been given to organotin(IV) azo-compounds particularly organotin azo-carboxylates for their various possible molecular architectures [13-18] and promising biological properties [15-18]. In recent years, organotin compounds with some functionalized azo-carboxylate ligands derived from 2- and 4-amino benzoic acids were studied extensively [19-22]. The antimicrobial and antidiabetic assays for these compounds were performed and found to exhibit significant activity. In addition to this, more recently we have also explored organotin (IV) compounds with some azo-carboxylate ligands derived from 2- and 4-amino benzoic acids and naphthalen-2-ol [23, 24]. The molecular structures of triorganotin (IV) compounds with these ligand systems were determined and structure of all the complexes showed five coordinated distorted trigonal bipyramidal geometry [23]. Furthermore, the crystal structures of dibutyltin (IV) compounds with these ligand systems were also determined and study of these structures revealed that the geometry around tin atoms adopted five coordinated distorted trigonal bipyramidal to six coordinated distorted octahedral or skew trapezoidal structures depending on the stoichiometric reaction ratios and type of the ligands employed [24]. Similarly, molecular structures and antidiabetic properties of organotin (IV) complexes with a new series of azo-carboxylate derived from 2- amino benzoic acid and naphthalen-1-ol were also studied [25]. The molecular structures of tributyltin and trimethyltin

(IV) complexes with this azo-carboxylate ligand exhibited distorted trigonal bipyramidal geometry while dibutyltin (IV) complex showed dinuclear structure with skew trapezoidal and pentagonal bipyramidal geometry around the two tin atoms in the dinuclear structure [25].Therefore, in continuation with our previous work in this research area, now we report herein three new triphenyltin (IV) compounds with these ligands *i.e.* azo-carboxylate ligands prepared from diazo-coupling reaction of 2 or 4-amino benzoic acids and naphtalen-1-ol or naphthalen-2-ol. In this present contribution, we have employed carboxylate ligands that have variation in the position of carboxylate functionality in the diazo-part (2 or 4- positions) and also varied the position of hydroxy group in the coupling moieties of the molecule (i.e. naphalen-1 or 2-ol). By using carboxylate functionality at different positions in the diazo-part and introducing a hydroxy group at different position in the coupling moieties, we would expect to afford organotin (IV) compounds with different structures which would influence their biological properties. Thus, considering all these facts, we have synthesized three new triphenyltin (IV) compounds using these ligands and the synthesized compounds were completely characterized by elemental analysis, IR and multinuclear (^{1}H, ^{13}C and ^{119}Sn)-NMR spectroscopy. The structures of compounds **1** and **3** were determined and the results are discussed and reported herein. In addition to this, Hirshfeld surface analysis for the structure of compounds **1** and **3** were also performed. Finally, all the synthesized compounds were screened for their antimicrobial activity and the results of the assay are discussed and compared with standard antibiotics.

2. Experimental

2.1 Materials and methods

2-aminobenzoic acid, 4-aminobenzoic acid, 1-naphthol, 2-naphthol and triphenyltin(IV) chloride were purchased from Merck and were used without further purification. Solvents were purified

and dried using standard procedure. Ph_3SnOH was synthesized from Ph_3SnCl using aqueous solution of NaOH following the standard procedure [26]. Elemental analysis was performed on Perkin Elmer 2400 series II instrument. Shimadzu FT-IR-8400S spectrophotometer in the range of 4000-400 cm^{-1} was employed for recording IR spectra with samples investigated using KBr discs. The NMR (^1H, ^{13}C) spectra for the compounds were recorded on a Bruker AMX 400 spectrometer and were measured at 400.13 and 100.62 MHz respectively whereas ^{119}Sn NMR spectra of the compounds were recorded on ECZR Series 600 MHz NMR spectrometer and measured at 223.75 MHz. ^1H and ^{13}C chemical shift was referenced to Me_4Si set at 0.00 ppm while Me_4Sn was employed as reference for ^{119}Sn chemical shifts and set at 0.00 ppm.

2.2. Synthesis

2.2.1. Synthesis of 2/4-(2-hydroxynaphthylazo) benzoic acid (H_2L^1 and H_2L^2) and 2-(4-hydroxynaphthylazo) benzoic acid (H_2L^3)

The azo carboxylate ligands *viz.* 2-(2-hydroxynaphthylazo) benzoic acid (H_2L^1), 4-(2-hydroxynaphthylazo) benzoic acid (H_2L^2) and 2-(4-hydroxynaphthylazo) benzoic acid (H_2L^3) were prepared by simple diazo-coupling reaction of 2-aminobenzoic acid or 4-aminobenzoic acid with naphthalen-1-ol or naphthalen-2-ol using our similar reported procedures [23, 25]. 2-(2-hydroxynaphthylazo)benzoic acid (H_2L^1)**:** red colour; Yield: 8.1 g, 76 %; m. p.: 260-262 °C; 4-(2-hydroxynaphthylazo)benzoic acid **(**H_2L^2**):** red colour; Yield: 8.5 g, 79 %; m. p.: 290-295 °C; 2-(4-hydroxynaphthylazo)benzoic acid **(**H_2L^3**):** deep red colour ; Yield: 6.9 g, 65 %; m. p.: 232-234°C. The structural formula and numbering scheme for the ligands H_2L^{1-3} are shown in **Scheme 1.**

<Scheme 1>

*2.2.2. Synthesis of Ph_3SnHL^1 (**1**)*

Triphenyltin(IV) compound **1** was synthesised by the reaction of 2-(2-hydroxynaphthylazo) benzoic acid with triphenyltin hydroxide in 1:1 (M: L) molar reaction ratio in anhydrous toluene using Dean-Stark apparatus. In this synthetic procedure, 2-(2-hydroxynaphthylazo) benzoic acid (0.2385 g, 0.8167 mmol) was dissolved in 50 mL anhydrous toluene with continuous stirring to yield a red coloured suspension. To that suspended solution, 0.3 g (0.8167 mmol) triphenyltin hydroxide was added and clear red coloured solution appeared immediately. The reaction mixture was then continued to refluxing for about 6 hours fitted with the Dean Stark apparatus. The solution was then filtered and the filtrate was kept for evaporation at room temperature to afford pure red crystals of the compound. Yield: 79 %; m. p.: 215-217 °C. Anal. found: C, 65.87; H, 4.19; N, 4.72%. Calc. for $C_{35}H_{26}N_2O_3Sn$: C, 65.55; H, 4.09; N, 4.37%. IR (KBr, cm^{-1}): 3450 ν(N-H), 1619 $\nu(COO)_{asym}$, 1478 ν(N=N), 1155 ν(C-O), 697 ν(Sn-C), 470 ν(Sn-O).^{1}H NMR ($CDCl_3$, 400.13 MHz) δ_H, Ligand skeleton: 8.41 [d, 1H, H-9, J = 8.0 Hz], 8.27 [d, 1H, H-3′, J = 8.4 Hz], 8.21 [d, 1H, H-6, J = 8.0 Hz], 8.03 [m, 1H, H-4], 7.88 [m, 1H, H-4′], 7.59 [m, 1H, H-6′ and H-8], 7.35 [t, 1H, H-5′, J = 7.6 Hz], 7.16 [t, 1H, H-7, J = 7.6 Hz], 6.71[d, 1H, H-3, J = 9.6 Hz]; Sn-Ph skeleton: 7.95 [m, 6H, H-*o*], 7.48 [m, 9H, H-*m* and H-*p*] ppm. ^{13}C NMR ($CDCl_3$, 100.62 MHz) δ_C, Ligand skeleton: 179.9 [COO], 172.9 [C-2],145.1 [C-1′], 141.9 [C-1], 134.45 [C-4], 134.2 [C-5′], 132.9 [C-4′], 131.4 [C-3′], 129.4 [C-10], 128.8 [C-5], 128.7 [C-6], 127.7 [C-8], 126.8 [C-9], 123.9 [C-7], 122.7 [C-6′], 117.2 [C-3], 116.5 [C-2′]; Sn-Ph skeleton: 138.7 [C-*i*], 137.5 [C-*o*] ^2J [$^{119/117}$Sn-^{13}C (48.8 Hz)], 130.4 [C-*p*] ^4J [$^{119/117}$Sn-^{13}C (13.3 Hz)], 129.1 [C-*m*] ^3J [$^{119/117}$Sn-^{13}C (64.7 Hz)] ppm. ^{119}Sn NMR ($CDCl_3$, 223.75 MHz): -104.7 ppm. The numbering scheme for triphenyltin skeleton is shown below:

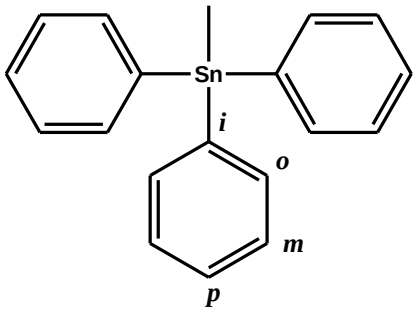

2.2.3. Synthesis of Ph_3SnHL^2 (**2**)

Compound **2** was synthesised following the analogous procedure as in case of compound **1** by the reaction of 4-(2-hydroxynaphthylazo)benzoic acid instead of 2-(2-hydroxynaphthylazo) benzoic acid with triphenyltin hydroxide in 1:1 (M: L) molar reaction ratio in anhydrous toluene using Dean-Stark apparatus. The solid product obtained from filtrate was recrystallized from anhydrous toluene to yield deep red crystalline product of compound **2**. Yield: 69%; m. p.: 182-184 °C. Anal. found: C, 65.37; H, 3.91; N, 4.18%. Calc. for $C_{35}H_{26}N_2O_3Sn$: C, 65.55; H, 4.09; N, 4.37 %. IR (KBr, cm^{-1}): 3410 *ν*(N-H), 1619 $\nu(COO)_{asym}$, 1485 *ν*(N=N), 1165 *ν*(C-O), 671 *ν*(Sn-C), 495 *ν*(Sn-O). ^{1}H NMR ($CDCl_3$, 400.13 MHz) δ_H, Ligand skeleton: 8.46 [d, 1H, H-9, *J* = 8.0 Hz], 8.22 [d, 2H, H-3′, H-5′, *J* = 8.8 Hz], 7.90 [m, 1H, H-4], 7.76 [m, 1H, H-6], 7.65 [m, 3H, H-2′, H-6′ and H-8], 7.39 [t, 1H, H-7, *J* = 7.2 Hz], 6.74 [d, 1H, H-3, *J* = 9.6 Hz]; Sn-Ph skeleton: 7.82 [m, 6H, H-*o*], 7.49 [m, 9H, H-*m* and H-*p*] ppm.^{13}C NMR ($CDCl_3$, 100.62 MHz) δ_C, Ligand skeleton: 177.7 [COO], 172.1 [C-2], 146.8 [C-1′], 142.2 [C-1], 133.6 [C-4], 132.6 [C-2′, C-6′], 131.1 [C-4′], 129.5 [C-10], 128.8 [C-5], 128.5 [C-8], 128.2 [C-9], 126.8 [C-7], 126.2 [C-6], 122.3 [C-3], 117.0 [C-3′ and C-5′]; Sn-Ph skeleton: 138.5 [C-*i*], 137.1 [C-*o*] ^2J [$^{119/117}$Sn-^{13}C (47.8 Hz)], 130.4 [C-*p*] ^4J [$^{119/117}$Sn-^{13}C (13.1 Hz)], 129.1 [C-*m*] ^3J [$^{119/117}$Sn-^{13}C (49.81 Hz)] ppm. ^{119}Sn NMR ($CDCl_3$, 223.75 MHz): - 109.8 ppm.

2.2.4. Synthesis of Ph_3SnHL^3 (**3**)

A similar synthetic procedure as described above as in case of compound **1** was followed for the synthesis of compound **3** where 2-(4-hydroxynsaphthylazo)benzoic acid was used as azo-carboxylate ligand instead of 2-(2-hydroxynaphthylazo) benzoic acid with triphenyltin (IV) hydroxide in 1:1 (M:L) molar reaction ratio in anhydrous toluene using the Dean-Stark apparatus. The compound was recrystallized from anhydrous toluene to get pure deep red crystals of compound **3**. Yield: 73 %; m. p.: 147-149 °C. Anal. found: C, 65.97; H, 4.79; N, 4.91 %. Calc. for $C_{35}H_{26}N_2O_3Sn$: C, 65.55; H, 4.09; N, 4.37%. IR (KBr, cm^{-1}): 3435 ν(N-H), 1623 $\nu(COO)_{asym}$, 1475 ν(N=N), 1155 ν(C-O), 733 ν(Sn-C), 506 ν(Sn-O). ^{1}H NMR ($CDCl_3$, 400.13 MHz) δ_H, Ligand skeleton: 12.59 [s, 1H, OH], 8.44 [d, 1H, H-9, J = 8.0 Hz], 8.18 [d, 2H, H-6, H-3′, J = 7.6 Hz], 7.97 [m, 1H, H-2], 7.89 [m, 1H, H-7], 7.74 [m, 1H, H-8], 7.64 [t, 1H, H-4′, J = 7.6 Hz], 7.54 [m, 1H, H-6′], 7.02 [t, 1H, H-5′, J = 8.0 Hz], 6.62 [d, 1H, H-3, J = 10.4 Hz]; Sn-Ph skeleton: 7.81 [m, 6H, H-*o*], 7.51 [m, 9H, H-*m* and H-*p*] ppm. ^{13}C NMR (DMSO-d_6, 100.62 MHz) δ_C Ligand Skeleton: 185.2 [COO], 174.0 [C-4], 145.6 [C-1′], 135.9 [C-1], 135.0[C-5′], 133.9 [C-10], 132.1 [C-3′], 132.3 [C-4′], 130.4 [C-6], 113.5 [C-3]; other signals: 130.1, 128.2, 126.2, 124.3, 123.1, 121.3, 114.4; Sn-Ph skeleton: 138.1 [C-*i*], 137.0 [C-*o*] ^2J [$^{119/117}$Sn-^{13}C (48 Hz)], 130.7 [C-*p*] ^4J [$^{119/117}$Sn-^{13}C (13.1 Hz)], 129.3 [C-*m*] ^3J [$^{119/117}$Sn-^{13}C (63.4 Hz)] ppm. ^{119}Sn NMR ($CDCl_3$, 223.75 MHz): - 102.1 ppm.

2.3. X-ray crystallography

Single crystal X-ray diffraction data were collected by the ω-scan technique using MoK_α (λ = 0.71073Å) radiation. Both crystals of compounds **1** and **3** were studied at 100(3) K using a RIGAKU XtaLAB Synergy, Dualflex, Pilatus 300K diffractometer [27] with Photon Jet micro-focus X-ray Source. Data collection, cell refinement, data reduction and absorption correction

were carried out using CrysAlis PRO software [27]. The crystal structures were solved by using direct methods with the SHELXT 2018/2 program [28]. Atomic scattering factors were taken from the International Tables for X-ray Crystallography. Positional parameters of non-H-atoms were refined by a full-matrix least-squares method on F^2 with anisotropic thermal parameters by using the SHELXL 2018/3 program [29]. Hydrogen atoms participating in hydrogen bonding were found on the Fourier map and freely refined while the other were placed in calculated positions (C–H = 0.93–0.98 Å) and included as riding contributions with isotropic displacement parameters set to 1.2-1.5 times the U_{eq} of the parent atom. Crystal data and structure refinement parameters are shown in **Table 1**, while selected geometric parameters are collected in **Table 2**.

<**Table 1**>

<**Table 2**>

2.4 Hirshfeld surfaces

The Hirshfeld surfaces (HS) [30] and the related 2D-fingerprint plots (FP) [31] were calculated using Crystal Explorer software ver. 17.5 [32]. An in-depth introduction to HS analysis has been described elsewhere [33]. The crystal data of **1** and **3** imported from CIF files were used for analysis. Before starting the calculations the bond lengths to hydrogen atoms were set to standardized neutron values (O–H= 0.983Å, N–H= 1.009Å and C–H= 1.083Å).

2.5. Antimicrobial assay

Compounds **1-3** and ligands [$\mathbf{H_2L^{1\text{-}3}}$] were screened for their antimicrobial activity following modified Kirby-Bauer-Disc-Diffusion Assay [34]. Antibacterial screening assays were performed using three bacterial species (*Escherichia coli*, *Pseudomonas aeruginosa* and *Staphylococcus aureus)*. For anti-fungal screening, two fungi (*Fusarium verticilloiodes* and

Fusarium chlamydosporum) were used for compounds **1** and **2** while *Fusarium oxysporum, Candida albicans and Penicillium chrysogenum* were employed for compound **3**. Samples solution were prepared by dissolving 1 mg of each sample in 20 µL DMSO and then solution was diluted up to 1 mg/mL using sterile distilled water. Standard antibiotics solution (1mg/ mL concentration) was also prepared as reference controls for both bacterial and fungal assays. Prior to the antimicrobial assay, all the experimental organisms were revived by streaking on specific agar media plates for fungi and in nutrient broth for bacteria. Bacterial inoculums were prepared by inoculating 150 µL of fresh culture (24 hour old) after diluting up to 1:4 ratios in nutrient broth. For preparing fungal inoculums, 150 µL of 7-days old fungal spore suspensions in sterile water (diluted to 1/5) was added to the vials containing the fungal cultures and the colonies were gently scraped out along with water and the suspension was vortexed at a minimum speed and used directly as inoculums. Filter paper discs (Whatmann No.1) of 6 mm diameter were prepared and sterilized by autoclaving prior to the assay. A thin layer of bacterial / fungal culture was prepared using L-spreader on the surface of Tomato Juice Agar, Plate Count Agar and King's B Agar media plates for bacteria; and Potato Dextrose Agar and Czapek Dox Agar media plates for fungi. The plates were dried for about 1 minute inside the laminar air flow chamber. Three filter paper discs previously saturated with test sample solutions (1mg/ mL) for screening and different doses for quantitative assay were placed on the surface of the bacterial / fungal culture plates. A standard antibiotic disc (conc. same as the test samples) of streptomycin / amphotericin B were also prepared for comparison. The plates were incubated for 24 hours at 37º C for bacteria and 72 hours at 30º C for fungi inside BOD incubator. The bacterial and fungal inhibition zones (mm) were recorded for all samples as well as for the standard antibiotics. For quantitative dose analysis, two bacterial species (*S.aureus* and *P. aeruginosa*) and two fungi (*F. oxysporum* and *P.*

chrysogenum) were employed. Concentrations of (25µg, 50µg, 100µg, 200µg, 500µg and 1000µg) in 1 mL were used for bacteria for all the samples against the bacterial pathogens. For fungal assay, the same concentration were also used for compounds **1** and **2** while for compound **3** different concentration (250µg, 500µg, 750µg, 1000µg and 1500µg) in 1 mL were tested. Inoculation procedure and incubation conditions were maintained same as described in screening test.

3. Results and discussion

3.1. Synthesis

Triphenyltin(IV) compounds **1**-**3** were synthesized by reacting 2-(2-hydroxynaphthylazo) benzoic acid [H_2L^1] (**1)** or 4-(2-hydroxynaphthylazo) benzoic acid [H_2L^2] (**2)** or 2-(4-hydroxynaphthylazo) benzoic acid [H_2L^3] (**3**) with triphenyltin (IV) hydroxide in anhydrous toluene using the Dean-Stark apparatus in 1:1 (M: L) molar reaction ratio. All the compounds were obtained in good yield, stable at room temperature and they are soluble in most of the common organic solvents. The reaction scheme for the synthesis of compounds **1**-**3** is shown in **Scheme 2**.

< Scheme 2>

3.2. Spectroscopic characterization

3.2.1. IR Spectroscopy

The IR spectroscopic data for the compounds were provided in experimental section while IR spectroscopic data for the azo-carboxylate ligands were reported in our earlier report [23, 25]. The azo-carboxylate ligands H_2L^{1-3} showed asymmetric [ν_{asy}(COO)] stretching absorption band at 1710, 1716 and 1673 cm^{-1} respectively while in case of compounds **1**-**3**, this IR stretching absorption bands was shifted to lower wave number in the range at 1619-1623 cm^{-1} which is in

consistent for the carboxylate coordination to tin- atom in the complexes [15, 17, 23]. The IR absorption bands observed in the range 671-733 cm^{-1} and 470-506 cm^{-1} of compounds **1-3** could be assigned for Sn-C and Sn-O respectively [19, 35, 36]. Moreover, broad IR absorption band observed around 3400 cm^{-1} in the compounds could be assigned for N-H stretching frequency [25].

3.2.2. Multinuclear (^{1}H, ^{13}C and ^{119}Sn) NMR spectroscopy

The synthesis and complete characterization data for the azo-carboxylate ligands used in this present work has been described in our previous work [23, 25]. The ^{1}H-, ^{13}C- and ^{119}Sn- NMR spectra for the triphenyltin compounds **1-3** were recorded in $CDCl_3$ and their spectroscopic data were assigned subsequently by comparing with the spectroscopic data of the corresponding azo-carboxylate ligands because of their data similarities. In proton NMR spectra of the compounds, the aromatic protons were observed in the range 6.67-8.37 ppm while triphenyltin protons in the compounds showed two multiplet peaks at 7.48-7.51 and 7.81-7.95 ppm. In ^{13}C NMR spectra of the compounds, the carbon signals for aromatic carbons appeared in the range 116.5-174.1 ppm while ^{13}C signals for (COO) were observed at around 177.7-185.2 ppm. Further, four ^{13}C-signals appeared in the range 129-139 ppm were assigned for the phenyl carbons; C-*ispo* (138.1-138.7), C-*ortho* (137.0-137.5), C-*para* (130.4-130.7) and C-*meta* (129.1-129.3) ppm respectively [18, 19, 37]. Moreover, the coordination behaviour around tin atoms in solution state can be investigated using ^{n}J [$^{119/117}$Sn-^{13}C] coupling constants and the corresponding observed ^{n}J [$^{119/117}$Sn-^{13}C] values for the triphenyltin (IV) compounds **1-3** were found to be in consistent with those compounds with 4-coordinated quasi-tetrahedral geometry reported in the literature [14, 18, 19, 37, 38]. Furthermore, ^{119}Sn -NMR spectroscopy study also used for confirming the geometry around tin atom in the complexes in solution state. ^{119}Sn chemical shift values for

compounds **1**- **3** were observed at -104.78, -109.88 and -102.12 ppm respectively indicating all the compounds adopted 4-coordinated tetrahedral structures in solution state [14, 18,19, 37-39]. Hence, it can be suggested that the 5-coordinated solid state structure of compound **1** is dissociated into four coordinated structure while the solid state structure of compound **3** is also retained in solution state (*vide infra* X-ray crystal structure).

3.3. Description of the crystal structures

The atomic numbering scheme and the coordination around the tin atom for the complexes **1** and **3** are illustrated in **Figs. 1** and **2**, respectively. Selected bond lengths and bond angles are listed in **Table 2**. In both structures **1** and **3**, the ligands occur in the hydrazone form. The complex Ph_3SnHL^1 (**1**) comprises discrete molecular units wherein the central Sn atom is five-coordinated to the three phenyl ligands and the chelated by carboxylate group. The almost equal Sn–C bond lengths [mean bond length Sn–C = 2.1263(18)Å] are consistent with those reported in the literature [40]. The C–Sn–C bond angles [C(18)–Sn(1)–C(24), C(18)–Sn(1)–C(30), C(24)–Sn(1)–C(30)] are 110.30(7)°, 108.94(7)° and 116.14(7)°, respectively and their sum of 335.41(7)° clearly differs from 360°. As is often seen in such complexes [41] the carboxylate is unsymmetrically bidentate. The two oxygen atoms are bonded to Sn atom with significantly different Sn–O distances of 2.0751(14)Å and 2.6472(12)Å respectively, according to the stronger coordinative ability of the carboxylate O atom than the carbonyl O atom. Longer weak Sn(1)–O(2) bond is considerably shorter than the sum of the van der Waals radii of the Sn and O atoms (3.68Å) [42] and should rather be considered as semi-coordinative but still of physical significance. The Sn coordination sphere deformation can be explained by the Berry pseudo-rotation mechanism [43] and characterized quantitatively by parameter τ defined by Addison et al. [44], (τ = 0.58; cf. the τ values for the idealized geometries are τ = 0, square planar, τ = 1,

trigonal bipyramidal). The parameter τ indicates intermediate deformation between the trigonal bipyramidal and square-pyramidal geometry. The intramolecular N-H···O hydrogen bonds [N(1)-H(1)···O(2) and N(1)-H(1)···O(3)] help to establish near planar conformation of molecule **(Table 2)**. Packing diagram of complex **1** is shown in **Fig. S4**. No other significant supramolecular interactions were found.

< Figure 1>

Like in structure **1**, the structure of **3** is also built from monomeric molecules, but the Sn atom has a distorted tetrahedral coordination geometry (**Fig. 2**). The coordination sphere involves the three phenyl ligands and the carboxylate O-atom of the **HL^3** ligand. The range of the tetrahedral angles at the Sn atom is 97.50(6)° to 122.19(6)°. The C–Sn–C angles are larger than the ideal tetrahedral value, probably due to the steric effects arising between the phenyl ligands. The carbonyl O(2) atom, interacts only weakly with the Sn-atom at a distance of 2.843(2)Å This interaction is the cause of the distortion of the tetrahedral primary coordination sphere, but the Sn(1)···O(2) distance is considered to be too long for the Sn atom to be described as truly five-coordinate. Similar distorted tetrahedral geometry around the Sn atom was observed in triphenyltin(IV) complex with 2-hydroxybenzoic acid derivative [45]. Due to the different location of the hydroxy group in ligand, only one intramolecular hydrogen bond of type N-H···O (Table 3) is observed in **3**. In addition the carbonyl O(2) atom also plays a role in stabilizing structure through interaction of type C-H···O (**Table 3, Fig. S5**).

< Table 3>

< Figure 2>

3.4. Hirshfeld surfaces analysis

The ligands $\mathbf{H_2L^1}$ and $\mathbf{H_2L^3}$ used for the synthesis of complexes differed in the position of the hydroxy group in the molecule. The impact of this difference on intermolecular interactions seemed interesting to analyze. For this reason the Hirshfeld surfaces (HS) and their associated two-dimensional fingerprint plots (FP) were used to quantify intermolecular interactions. The 3D Hirshfeld surfaces of the title compounds are illustrated in **Figure 3**, with maps d_{norm} and shape index. The red spots on d_{norm} correspond to the dominant intermolecular interactions in the crystals. The contributions of specific types of contacts to the Hirshfeld surfaces for compounds **1** and **3** have been summarized in **Table 4 and Figure S6.** Both, in structure **1** and **3** van der Waals forces (H···H and C···H/H···C contacts) constitute the majority of forces contributing to the stacking of the molecules in the structures. In structure **1** due to the involvement of two oxygen atoms in intramolecular hydrogen bonds higher contribution of C···C contacts of 9.0 %, than H···O/O···H contacts of 7.1% is observed. The reverse situation is seen in structure **3** where C···C and H···O/O···H contacts are 5.0 % and 7.1% respectively. This difference shows the greater importance of stacking interactions in crystal packing of **1** than in **3**.

< Figure 3>

3.5. Antimicrobial activity studies

The antimicrobial activity of all the synthesized compounds **1-3**, tin starting material Ph_3SnOH and the ligands were evaluated by screening against three bacterial and five fugal species. The results of the antimicrobial screening test of the compounds, Ph_3SnOH and the ligands along with the standard compounds streptomycin for anti-bacterial test and amphotericin B / ampicillin for antifungal test as reference controls are listed in **Table 5**. Quantitative dose analysis for compounds **1-3** and standard compounds were also studied against two bacteria (*S. aureus* and *P.*

aeruginosa) and two fungi (*F. oxysporum* and *P. chrysogenum)*. The results of the quantitative assay of the compounds along with standard compounds are listed in **Table 6**. From dose quantitative study, it is seen that, in general the antibacterial activity of compounds **1-3** and standard compound streptomycin increases with increase in concentration (from 25 to 1000 μg/mL) of the tested compounds. They showed maximum activity at 500 or 1000 μg/mL against *S. aureus.* Compound **3** was found to be the most effective antibacterial agent at 1000 μg/mL (17.7 mm) and exhibited activity higher than streptomycin (11.6 mm) at the same concentration against *S.aureus*. The tin starting material Ph_3SnOH exhibited lower antibacterial activity as compared to the compounds at higher concentration but did not show activity at lower concentration against *S. aureus*. Compounds **1** and **3** showed higher antibacterial activity than standard compound streptomycin against *S.aureus*. However, all the tested compounds did not show any antibacterial activity at different dose against *P. aeruginosa.* Furthermore, antifungal dose quantitative assay against *F. oxysporum* showed that the antifungal activity of the compounds generally increases with increase in concentration up to certain optimum concentration, and then activity decreases with increase in concentration (**Table 6**). Compounds **1** and **2** showed higher antifungal activity than compound **3** and the standard compound amphotericin B against *F. oxysporum*. However, compounds **1** and **2** did not show any antifungal activity against *P. chrysogenum* but compound **3**, the tin starting material and amphotericin B were found to exhibit antifungal activity against this fungus. The antimicrobial activity of these compounds may be explained on the basis of the formation of hydrogen bonding through hydroxy group with the active center of the cell constituents which consequently interfere with the normal cell processes [46]. Furthermore, the antimicrobial activity of triphenyltin (IV) compounds can be attributed to the presence of bulky phenyl groups which can

facilitate the binding to biological molecules through π-π interactions [13]. The results of the antimicrobial activity study of all the screened microbes for the present triphenyltin (IV) compounds could not be compared with those of the similar type of triphenyltin (IV) compounds with azo-carboxylates reported earlier because of the different methodologies and strains employed [47]. However, the antimicrobial activity of the present triphenyltin (IV) compounds against the tested bacteria, *S. aureus* and fungus, *F. oxysporum* were comparable with the reported tributyltin (IV) compounds of the similar ligands [23]. Few compounds were also found to exhibit activities higher than the standard antibiotics, streptomycin and amphotericin against few selected tested microbes.

4. Conclusions

Three triphenyltin(IV) complexes **1-3** were synthesized by reacting three azo-carboxylic acid ligands *viz*.2/4-(2-hydroxynaphthylazo)benzoic acids or 2-(4-hydroxynaphthyl azo)benzoic acid with triphenyltin(IV) hydroxide. The compounds were characterized by elemental analysis, IR and multinuclear NMR spectroscopy. The molecular structure of **1** and **3** was determined by X-ray crystal structure analysis. In complex **1**, the coordination sphere of Sn atom showed intermediate deformation between the trigonal bipyramidal and square-pyramidal geometry, while in **3** distorted tetrahedral geometry around tin atom is observed. Intra-molecular hydrogen bonding between N-H...O were also present in both the structures. Hirshfeld surfaces analysis was performed for the structure of compounds **1** and **3**. The main difference between **1** and **3** is observed for stacking interactions. NMR spectral study indicated that all the compounds adopted four coordinated tetrahedral structures in solution. Thus five coordinated solid state structure of compound **1** is suggested to dissociate into four coordinated structure while solid state structure

for compound **3** is also retained in solution. All tested compounds showed effective antibacterial activity against *S. aureus* and significant antifungal activity against fungi *F. oxysporum*. Compounds **1** and **3** showed higher antibacterial activity than standard compound streptomycin against *S. aureus* while compounds **1** and **2** were found to display higher antifungal activity than the standard antibiotic amphotericin B against *F. oxysporum*. Since the antimicrobial activity of few compounds of the present series showed higher activity than the tested standard compounds against few microbes, these compounds could be further studied to enhance antimicrobial therapeutic properties.

Acknowledgements

Authors would like to thank IISc, Bangalore for NMR spectra and DBT, Govt. of India (Grant No. BT/32/NE/2011) for Biotech Hub, Department of Forestry.

Supplementary materials

CCDC No. 2002480 and 2002481 contain the supplementary crystallographic data for compounds **1** and **3** receptively. These data can be obtained free of charge from The Cambridge Crystallographic Data Centre via www.ccdc.cam.ac.uk/data_request/cif.

References

[1**]** G. Prabusankar, R. Murugavel, Organometallics 23 (2004) 5644.

[2] E.R.T. Tiekink, Appl. Organomet. Chem. 5 (1991) 1.

[3] C. Ma, J. Sun, Dalton Trans. (2004) 1785.

[4] C. Ma, Z. Guo, R. Zhang, Polyhedron 27 (2008) 420.

[5] A.S. Sougoule, Z. Mei, X. Xiao, C.A. Balde, S. Samoura, A. Dolo, D. Zhu, J. Organomet. Chem. 19 (2014)758.

[6] E.R.T. Teikink, Trends Organomet.Chem. 1 (1994) 71.

[7] R. Garcı´a-Zarracino, H. Hopfl, J. Am. Chem. Soc. 127 (2005) 3120.

[8] V. Dokouro, A. Primikiri, D.K. Dimertzis, J. Inorg. Biochem. 105 (2011) 195.

[9] D.K. Dimertzi, V. Dokouro, A. Primikiri, R. Vergas, C. Silvestru, U. Russo, M.A. Dimertzis, J. Inorg. Biochem. 103 (2009) 738.

[10] M. Gielen, Appl. Organomet. Chem. 16 (2002) 481.

[11] M. Gielen, M. Biesemans, D. de Vos, R. Willem, J. Inorg. Biochem.79 (2000)139.

[12] D. Tzimopoulos, I. Sanidas, A.C. Varvogli, A. Czapik, M. Gdaniec, E. Nikolakaki, P.D. Akrivos, J. Inorg. Biochem. 104 (2010) 423.

[13] T.S. Basu Baul, A. Churasia, A. Duthie, P.M. Tolentino, H. Hopfl, Cryst. Growth Des. 19 (2019) 6656.

[14] T.S. Basu Baul, K.S. Singh, M. Holcapeck, R. Jirasko, E. Rivarola, A. Linden, J. Organomet. Chem. 690 (2005) 4232.

[15] T.S. Basu Baul, K.S. Singh, X. Song, A. Zapata, G. Eng, A. Lycka, A. Linden, J. Organomet. Chem. 689 (2004) 4702.

[16] T.S. Basu Baul, W. Rynjah, R. Willem, M. Biesemans, I. Verbruggen , M. Holcapek, D. de Vos, A. Linden, J. Organomet. Chem. 689 (2004) 4691.

[17] T.S. Basu Baul, K.S. Singh, A. Lycka, A. Linden, X. Song, A. Zapata, G. Eng, Appl. Organomet. Chem. 20 (2006) 788.

[18] T.S. Basu Baul, A. Paul, L. Pellerito, M. Scopelliti, A. Duthie, D.de Vos, R.P. Verma, U. Englert, J. Inorg. Biochem. 107 (2012) 119.

[19] M. Roy, S.S. Devi, S. Roy, C.B. Singh, K.S. Singh, Inorg. Chim. Acta 426 (2015) 89 .

[20] M. Roy, S. Roy, K.S. Singh, J. Kalita, S.S. Singh, Inorg. Chim. Acta 439(2016) 164.

[21] M. Roy, S. Roy, K.S. Singh, J. Kalita, S.S. Singh, New J. Chem. 40 (2016) 1471.

[22] M. Roy, S. Roy, N.M. Devi, C.B. Singh, K.S. Singh, J. Mol. Struct. 1119 (2016) 64.

[23] P. Debnath, A. Das, K.S. Singh, T. Yama, S.S. Singh, R.J. Butcher, L. Sieroń, W. Maniukiewicz, Inorg. Chim. Acta 498 (2019) 119172.

[24] P. Debnath, K.S. Singh, K.K. Singh, S.S. Singh, L. Sieroń, W. Maniukiewicz, New J. Chem. 44 (2020) 5862.

[25] P. Debnath, K.S. Singh, T.S. Devi, S.S. Singh, R.J. Butcher, L. Sieroń, W. Maniukiewicz, Inorg. Chim. Acta 510 (2020) 119736 .

[26] B. Kushlefsky, I. Simmons, A. Ross, Inorg. Chem. 2 (1963) 187.

[27] Rigaku OD. CrysAlis PRO. Rigaku Oxford Diffraction Ltd, Yarnton, Oxfordshire, England, 2019.

[28] G.M. Sheldrick, "SHELXT - integrated space-group and crystal-structure determination", Acta Cryst. A71 **(**2015) 3.

[29] G.M. Sheldrick, "Crystal structure refinement with SHELXL" Acta Cryst. C71 **(**2015) 3.

[30] M.A. Spackman, D. Jayatilaka, CrystEngComm 11 (2009) 19.

[31] M.A. Spackman, J.J. McKinnon, CrystEngComm 4 (2002) 378.

[32] M.J. Turner, J.J. McKinnon, S.K. Wolff, D.J. Grimwood, P.R. Spackman, D. Jayatilaka M. A. Spackman, CrystalExplorer ver. 17.5 (2017), University of Western Australia

[33] J.J. McKinnon, M.A. Spackman and A.S. Mitchell, Science, 60 (2004) 627.

[34] J. Hudzicki, Kirby-Bauer Disk Diffusion Susceptibility Test Protocol, American Society for Microbiology(https://www.asm.org/Protocols/Kirby-Bauer-Disk-Diffusion-Susceptibility-Test-Pro), (2009).

[35] C. Pettinari, F. Marchetti, R. Pettinari, D. Martini, A. Drozdov, S. Troyanov, Inorg. Chim. Acta 325 (2001) 103.

[36] A. Chilwal, G. Deep, P. Malhotra, A.K. Narula, J. Coord. Chem. 66 (2013) 1046.

[37] T.S. Basu Baul, A. Paul, A. Linden, J. Organomet. Chem. **696**, (2012), 4229.

[38] R. Willem, I. Verbruggen, M. Gielen, M. Biesemans, Mahieu, T.S. Basu Baul, E.R.T. Tiekink, Organometallics 17 (1998) 5758.

[39] M. Nadvornik, J. Holecek, K. Handlir, A. Lycka, J. Organomet. Chem. 43 (1984) 275.

[40] X. Xiao, Y. Li, Y. Dong, W. Li, K. Xu, N. Shi, X. Liu, J. Xie, P. Liu, J. Mol. Struct. 1130 (2017) 901.

[41] C. Camacho-Camacho, V.M. Jimenez-Perez, J.C. Galvez-Ruiz, A. Flores-Parra, R. Contreras, J. Organomet. Chem. 691 (2006) 1590.

[42] A. Bondi, J. Phys. Chem. 68 *(*1964) 44.

[43] R.S. Berry, J. Chem. Phys. 32 (3), (1960) 933.

[44] A.W. Addison, T.N. Rao, J. Reedijk, J. van Rijn, G.C. Verschoor, J. Chem. Soc., Dalton Trans., (1984), 1349.

[45] T.S. Basu Baul, W. Rynjah, E. Rivarola, A. Linden, J. Organomet. Chem. 690 (2005) 613.

[46] R.S. Srivastava, Inorg. Chim. Acta 56 (1981) L65.

[47] K.S. Singh, M. Roy, S. Roy, B. Ghosh, N.M. Devi, C.B. Singh, L.K. Mun, J. Coord. Chem.70 (2017) 361.

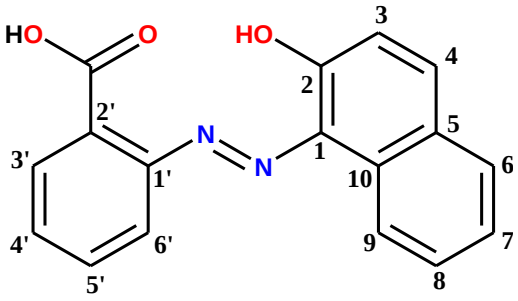

2-(2-hydroxynaphthylazo) benzoic acid ($\mathbf{H_2L^1}$)

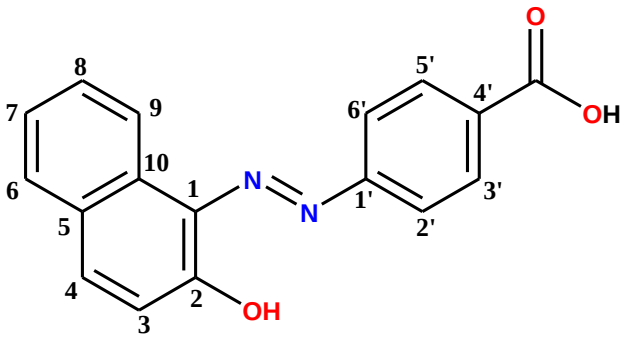

4-(2-hydroxynaphthylazo) benzoic acid ($\mathbf{H_2L^2}$)

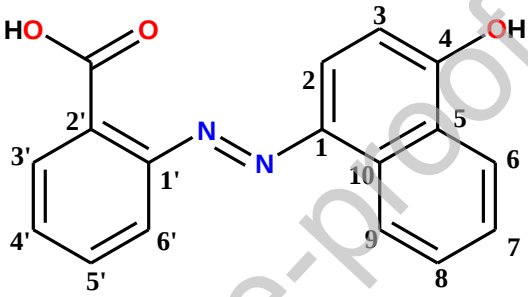

2-(4-hydroxynaphthylazo) benzoic acid ($\mathbf{H_2L^3}$)

Scheme 1. The structural formula and numbering scheme for the azo-carboxylate ligands $\mathbf{H_2L^1}$, $\mathbf{H_2L^2}$ and $\mathbf{H_2L^3}$.

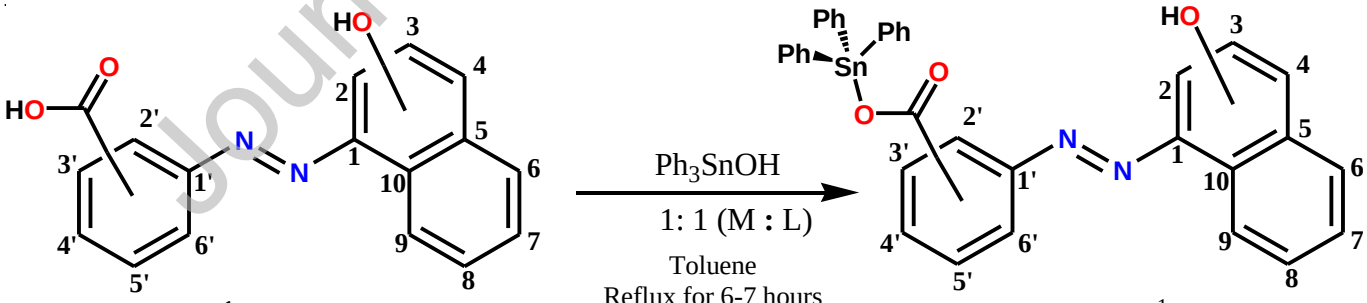

$\mathbf{H_2L^1}$: 2'-COOH, 2-OH
$\mathbf{H_2L^2}$: 4'-COOH, 2-OH
$\mathbf{H_2L^3}$: 2'-COOH, 4-OH

Ph_3SnHL^1 (**1**)
Ph_3SnHL^2 (**2**)
Ph_3SnHL^3 (**3**)

Scheme 2. Reaction scheme for the synthesis of triphenyltin (IV) compounds **1- 3**.

Table 1. Crystal data and structure refinement parameters for compounds **1** and **3**.

Parameters	**1**	**3**
Empirical formula	$C_{35}H_{26}N_2O_3Sn$	$C_{35}H_{26}N_2O_3Sn$
Formula weight	641.29	641.29
Temperature (K)	100(3)	100(3)
Wavelength (Å)	0.71073	0.71073
Crystal system	monoclinic	triclinic
Space group	$P2_1/c$	P-1
a (Å)	16.1609(2)	11.1879(1)
b (Å)	10.2454(1)	11.5828(1)
c (Å)	18.1466(2)	11.9869(1)
α (º)	90	103.979(1)
β (º)	113.908(1)	100.590(1)
γ(º)	90	103.737(1)
Volume ($Å^3$)	2746.82(6)	1415.51(3)
Z	4	2
Density (Mg/m^3)	1.551	1.505
Absorp. coeff. (mm^{-1})	0.971	0.942
F(000)	1296	648
Crystal size (mm^3)	0.35 x 0.60 x 0.65	0.16 x 0.19 x 0.60
Theta range for data collection	2.8, 25.0	2.9, 25.0
Index ranges	-19<=h<=19; -12<=k<=12; -21<=l<=21	-13<=h<=13; -13<=k<=13 -14<=l<=14
Reflection collected	147481	38945
Independent reflections	4851 [R(int) = 0.033]	5010 [R(int) = 0.027]
Goodness of fit on F^2	1.13	1.05
Final R indices [I>2sigma (I)]	0.0177	0.0152
R indices (all data)	0.0179	0.0156
Largest diff. peak and hole ($eÅ^{-3}$)	0.34 and -0.28	0.32 and -0.25

Table 2 Selected bond lengths (Å) and bond angles (º) for compounds **1** and **3**.

Atoms	**1** Bond Length (Å)	**3** Bond Length (Å)
Sn(1)-O(1)	2.0751(14)	2.0555(11)
Sn(1)-O(2)	2.6472(12)	-
Sn(1)-C(18)	2.1317(17)	2.1213(16)
Sn(1)-C(24)	2.1224(18)	2.1203(16)
Sn(1)-C(30)	2.1248(19)	2.1212(15)
Atoms	**1** Bond Angle (º)	**3** Bond Angle (º)
O(1)-Sn(1)-O(2)	54.08(5)	-
O(1)-Sn(1)-C(18)	97.03(6)	95.72(5)
O(1)-Sn(1)-C(24)	110.57(6)	108.37(5)
O(1)-Sn(1)-C(30)	112.19(6)	105.21(5)
O(2)-Sn(1)-C(18)	151.05(6)	-
O(2)-Sn(1)-C(24)	82.16(5)	-
O(2)-Sn(1)-C(30)	86.77(6)	-
C(18)-Sn(1)-C(24)	110.30(7)	109.59(6)
C(18)-Sn(1)-C(30)	108.94(7	112.24(6)
C(24)-Sn(1)-C(30)	116.14(7)	122.19(6)

Table 3 Hydrogen bonding parameters for compounds **1** and **3**

Compound	**D–H…A**	**d(D–H)**	**d(H…A)**	**d(D…A)**	**<(DHA)**
1	N(1)-H(1)…O(2)	0.85(2)	2.07(2)	2.692(2)	129(2)
	N(1)-H(1)…O(3)	0.85(2)	1.96(2)	2.616(2)	133(2)
3	N(1)-H(1)…O(2)	0.82(2)	1.98(2)	2.6586(18)	140(2)
	C(28)-H(28)…O(2)$^{\#1}$	0.95	2.59	3.450(2)	151

Symmetry code: (#1) 1-x,-y,1-z

Table 4 Summary of the various contact contributions (in %) in Hirshfeld surface area for all analyzed structures.

Contact type /Structure	**1**	**3**
H···H	49.8	46.6
C···H/H···C	30.2	35.3
O···H/H···O	7.1	9.3
C···C	9.0	5.0
N···C/C···N	-	1.5
N···H/H···N	2.4	1.4
O···C/C···O	0.8	0.4
N···N	0.6	-
O…N/N…O	-	0.5

Table5. Antimicrobial screening test for azo-carboxylate ligands and compounds (zone of inhibition in mm)

Ligands/ Compounds	Bacteria			Fungi				
	E. coli	*S. aureus*	*P. aeroginosa*	*F. verticiliodes*	*F. chlamydosporium*	*F. oxysporum*	*C. ablicans*	*P. chrysogenum*
H_2L^1	-	-	-	-	-	-	-	-
H_2L^2	-	-	-	-	-	-	-	-
H_2L^3	-	-	-	-	-	-	-	-
1	-	15.5	-	8.7	18.6	*	*	*
2	-	15.2	-	13.7	12.7	*	*	*
3	-	23.0	14.0	*	*	5.0	-	12.3
Ph_3SnOH	-	22.0	15.0	*	*	2.0	-	4.6
Streptomycin	10.5	11.0	10.3	*	*	*	*	*
Amphotericin-B	*	*	*	*	*	4.0	12.6	5.3
Ampicilin	*	*	*	-	-	*	*	*

(-) = Not active; (*) = Not tested

Table 6. Results of quantitative assay for the compounds and standard antibiotics against bacteria and fungi (in mm)

Compounds/standard antibiotics	Dose conc. for bacteria (in µg/mL)	Bacteria		Dose conc. for fungi (in µg/mL)	Fungi	
		S. aureus	*P. aeroginosa*		*F. oxysporum*	*P. chrysogenum*
1	25	6.9	-	25	5.6	-
	50	7.7	-	50	12.3	-
	100	8.2	-	100	11.8	-
	200	12.6	-	200	17.5	-
	500	11.0	-	500	20.2	-
	1000	12.7	-	1000	17.4	-
2	25	4.4	-	25	-	-
	50	4.6	-	50	7.6	-
	100	7.1	-	100	10.4	-
	200	8.6	-	200	15.6	-
	500	9.8	-	500	18.1	-
	1000	9.5	-	1000	18.2	-
3	25	4.3	-	-	2.4	-
	50	5.7	-	250	4.3	2.5
	100	6.6	-	500	5.0	3.6
	200	12.3	-	750	4.9	4.2
	500	16.5	-	1000	4.7	5.3
	1000	17.7	-	1500	2.4	7.0
Ph_3SnOH	25	-	-	-	-	-
	50	-	-	250	-	8.0
	100	-	-	500	-	7.6
	200	-	-	750	-	7.1
	500	4.0	-	1000	5.3	7.9
	1000	7.9	-	1500	-	10.6
Streptomycin	25	4.2	-	-	*	*
	50	5.2	-	250	*	*
	100	8.6	3.5	500	*	*
	200	9.5	3.6	750	*	*
	500	10.0	9.3	1000	*	*
	1000	11.6	6.3	1500	*	*
Amphotericin-B	25	*	*	-	-	-
	50	*	*	250	-	4.1
	100	*	*	500	-	7.2
	200	*	*	750	-	6.2
	500	*	*	1000	-	5.9
	1000	*	*	1500	5.7	6.0

(-) = Not active; (*) = Not tested

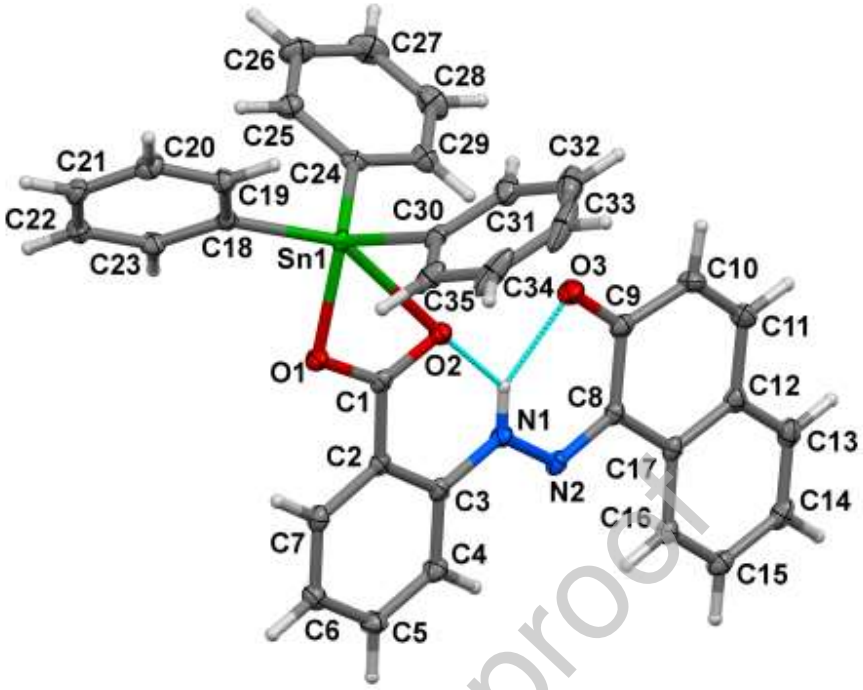

Fig. 1 The molecular structure of **1**. Displacement ellipsoids drawn at 50% probability level.

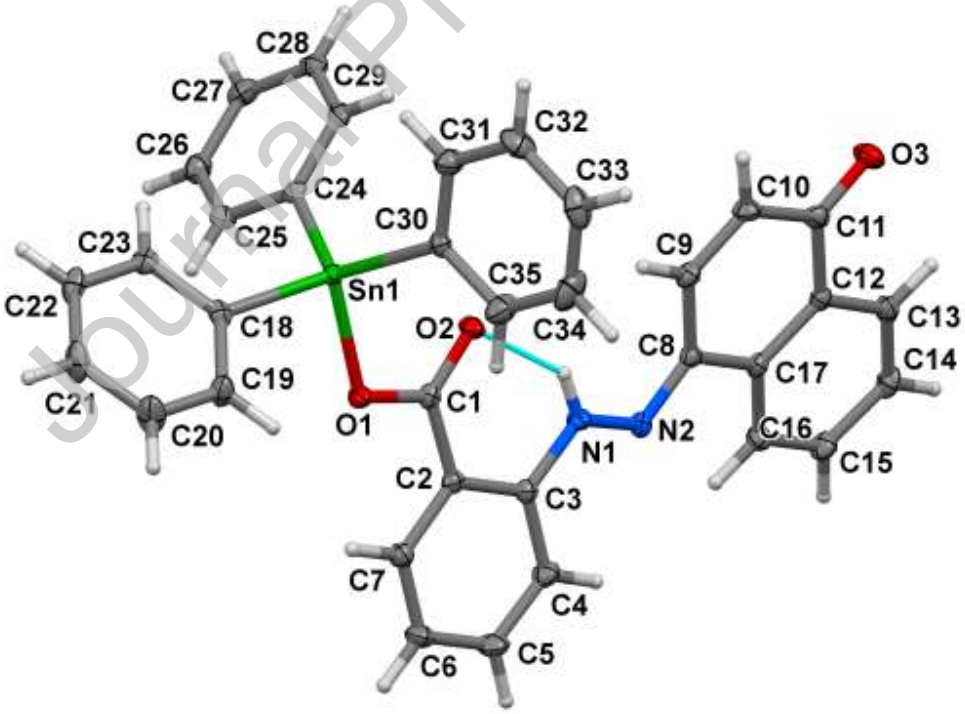

Fig 2. The molecular structure of **3**. Displacement ellipsoids drawn at 50% probability level

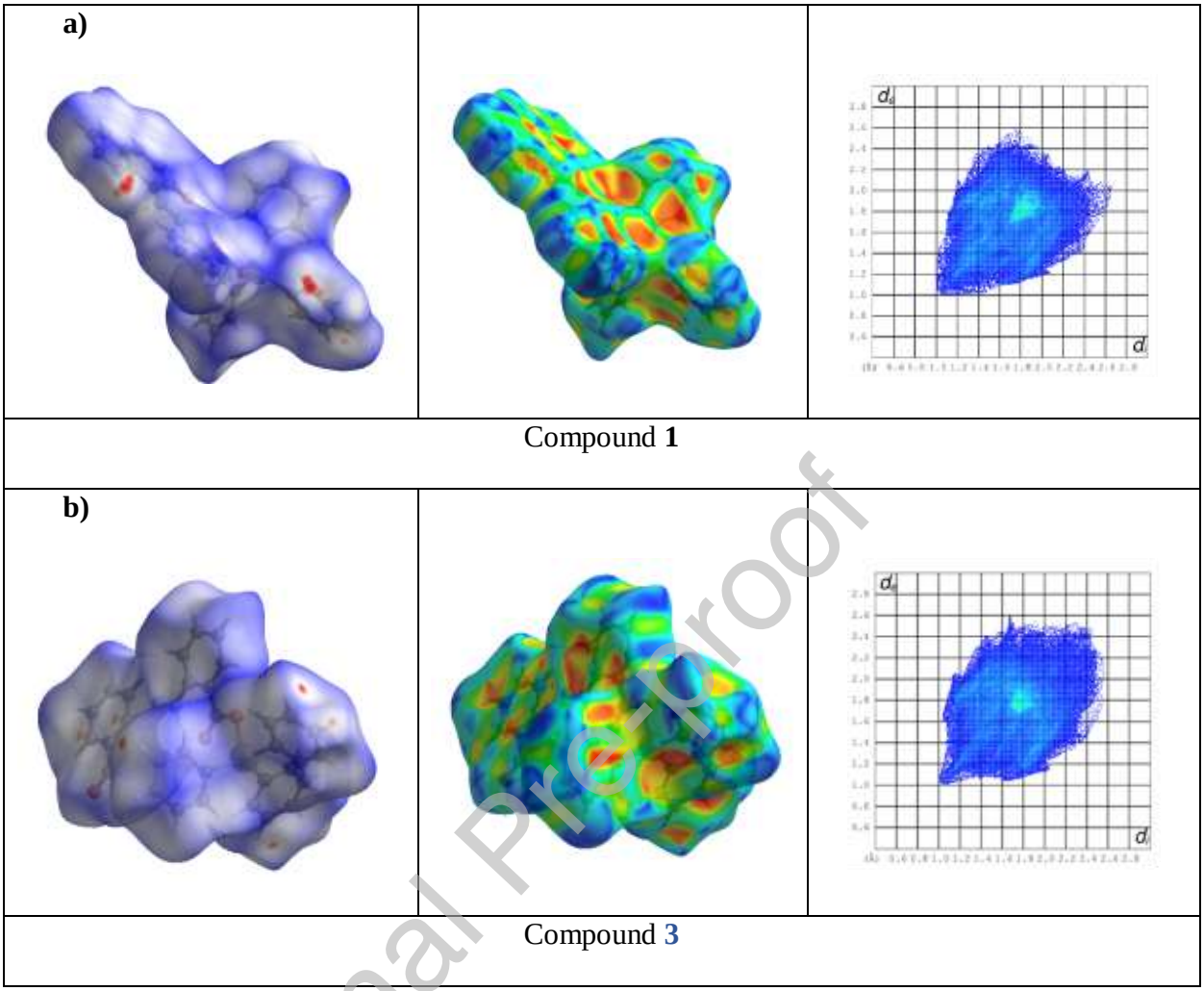

Fig. 3 Hirshfeld surfaces, shape-index surface and fingerprint plot of compounds **1** (a), and **3** (b) that are mapped with d_{norm} (left column), shape-index (middle column) and full fingerprint plot (right column).

Credit Author's Statement

Paresh Debnath: Methodology, Writing - original draft. Formal analysis. **Keisham Surjit Singh**: Supervision. Conceptualization. Writing - reviewing and editing. **Swatika Sharma**: Data Curation, Investigation. **Pratima Debnath:** Data Curation, Investigation **S.Sureshkumar Singh**: Formal analysis, Investigation. **Lesław Sieroń**.: Investigation. Visualization. **Waldemar Maniukiewicz**: Writing - original draft. Writing - review and editing.

Declaration of interests

☒ The authors declare that they have no known competing financial interests or personal relationships that could have appeared to influence the work reported in this paper.

☐The authors declare the following financial interests/personal relationships which may be considered as potential competing interests:

GRAPHICAL ABSTRACT